ELSEVIER

Biochimica et Biophysica Acta 1368 (1998) 289–305

BIOCHIMICA ET BIOPHYSICA ACTA
BBA

A model of hydrogen bond formation in phosphatidylethanolamine bilayers [1]

David A. Pink [a,*], Stew McNeil [a], Bonnie Quinn [a], Martin J. Zuckermann [b]

[a] *TPI, St. Francis Xavier University, P.O. Box 5000, Antigonish, Nova Scotia, Canada B2G 2W5*
[b] *Centre for the Physics of Materials, Department of Physics, McGill University, 3600 University Street, Montreal, Quebec, Canada H3A 2T8*

Received 15 July 1997; accepted 6 August 1997

Abstract

We have modelled hydrogen bond formation in phospholipid bilayers formed, in excess water, from lipids with phosphatidylethanolamine (PE) headgroups. The hydrogen bonds are formed between the NH_3^+ group and either of the PO_2^- or the (*sn2* chain) C=O groups. We used a model that represented the conformational states accessible to a PE headgroup by 17 states and modelled lipid dipole–dipole interactions using a non-local electrostatics theory to include the effects of hydrogen bonding in the aqueous medium. We used Monte-Carlo simulation to calculate equilibrium thermodynamic properties of bilayers in the fluid ($T = 340$ K) or gel ($T = 300$ K) phases of the bilayer. We defined E_h to be the difference in free energy between a hydrogen bond formed between a pair of lipid groups, and the energy of hydrogen bonds formed between water and those two groups, and we required its average value, $\langle E_h \rangle$, to be ~ -0.3 kcal/mol ($\sim -0.2 \times 10^{-13}$ erg) as reported by T.-B. Shin, R. Leventis, J.R. Silvius, Biochemistry 30 (1991) 7491. We found:

(i) $E_h = -0.9 \times 10^{-13}$ erg gave $\langle E_h \rangle = -0.21 \times 10^{-13}$ erg (gel phase) and $\langle E_h \rangle = -0.19 \times 10^{-13}$ erg (fluid phase).

(ii) The relative number of C=O groups on the *sn2* chain calculated to take part in interlipid hydrogen bonding in the fluid phase compared to the gel is 1.06 which compares well with the experimental ratio of ~ 1.25 (R.N.A.H. Lewis, R.N. McElhaney, Biophys. J. 64 (1993) 1081). The ratio of such groups taking part in interlipid hydrogen bonding compared to water hydrogen bonding in each phase was calculated to lie between 0.16 and 0.17.

(iii) We calculated the distribution of positions of the headgroup moieties, P, O, $CH_2(\alpha)$, $CH_2(\beta)$ and N, and found that, in both phases, the O lay furthest from the hydrocarbon chain layer (average ~ 5.3 Å) with the PO_2 and NH_3 groups lying at ~ 5 Å. This results in the P–N dipole lying nearly parallel to the bilayer plane in both phases. The thickness of the headgroup layer underwent essentially no change on going from the gel to the fluid phase. The ^{2}H NMR quadrupole splittings for the α and β CH_2 groups were 4.9 and 5.7 kHz (fluid phase) and 7.1 and 7.3 kHz (gel phase), respectively, on the assumption of sufficiently rapid rotation around the *z*-axis.

(iv) In both phases, the location of the NH_3^+ group exhibited a strong peak around 5.2 Å into the aqueous medium, with much smaller peaks around 2.6 and 7.8 Å, the two CH_2 groups exhibited narrower, double-peaked distributions and the O and the PO_2^- each exhibited a narrow single peak.

(v) PE headgroups, in a homogeneous gel phase, exhibited dipolar orientational long-range order in the plane of the

* Corresponding author. Fax: +1 902 867 2414; E-mail: dpink@juliet.stfx.ca

[1] Work supported by NSERC of Canada (DAP, SM and MJZ) and the UCR St. Francis Xavier University (SM).

PII S0005-2736(97)00196-X

bilayer. The distribution of orientation angles exhibited a full width at half height of between $\sim 40°$ and $\sim 50°$. In a fluid phase no such order was observed.
(vi) The number of hydrogen bonds did not differ substantially between the fluid and gel phases. This model is unlikely to display any significant effect of hydrogen bonding upon the ''main'' hydrocarbon chain melting phase transition at T_m, except, possibly, a broadening of any hysteresis, compared to the case of PC bilayers where interlipid hydrogen bonding is absent.

Keywords: Lipid bilayer; Hydrogen bond; Monte-Carlo computer simulation; Electrostatics

1. Introduction

The modelling of biological membranes has become the subject of enormous interest because of the insight that it might give into biological processes. One area of great interest has been to model biological membranes or lipid-bilayer membranes on a molecular scale, the characteristic length and time-scales of which are $\sim 10^{-1}$–10^{1} nm and $\sim 10^{-5}$ to $\sim 10^{-10}$ s, respectively. Such studies encompass, for example, phase transitions in lipid bilayers, the effects of lipid–protein interactions and ion transport through membranes [1]. An aspect of such systems, which has received much theoretical attention in recent years, has been the lipid–water interface of a lipid-bilayer membrane, or a lipid monolayer at an air–water interface. This interface is characterized by the presence of electric charges and electric dipoles located in the headgroups of phospholipid molecules, one of the principle components of some biological membranes [2]. Here, we shall be concerned with electrically neutral lipids possessing phosphatidylethanolamine (PE) headgroups. The headgroups are short chains which can adopt a number of different conformations. It is at such an interface that complex electrostatic fields can arise and these might play dominant roles in the conformations which water-soluble proteins might adopt at such an interface [3]. Because they are due to electric dipoles in an aqueous medium, such fields are of relatively short range and can be highly anisotropic. The different conformations available to the short dipolar chains admits, therefore, the possibility that biological membrane components arrange themselves so as to create local electric-field distributions suited for membrane function. In addition to electric dipoles, the possibility of both lipid–lipid and lipid–protein hydrogen bonding exists. This interaction, too, is highly anisotropic and short-ranged and cannot be ignored in certain membranes, especially when proteins are involved [3]. It is known that lipids with phosphatidylethanolamine (PE) headgroups take part in hydrogen bonding, with both water and other PE lipids, via their NH_3^+, PO_2^- and C=O moieties [4]. The third major interaction in membranes is the van der Waals interaction, relatively long-ranged and isotropic. In this paper, we shall model hydrogen bonding in phosopholipid bilayers, formed in excess water, in order to understand the interplay between hydrogen bonding and lipid headgroup conformational states, in the presence of headgroup dipole–dipole interactions [1–13].

Two approaches have been used to model phospholipid membranes: the use of molecular dynamics (MD), and related techniques [14–22] and the use of ''minimal'' models for which either Monte-Carlo (MC) or (exact or approximate) analytical methods can be employed [23–29]. The advantage of using ''minimal'' models is that, if their reliability has been established, they can be used to study large, complex systems. Here, we shall take this approach: We shall outline a simple model of the headgroup region of a phospholipid-bilayer membrane composed of lipid molecules with phosphatidylethanolamine (PE) headgroups, which takes into account those conformational states which do not violate steric constraints. We shall then combine this with a model of electrostatics of an aqueous solution which goes beyond Gouy–Chapman theory in that it takes into account, in an average way, the dynamic hydrogen bonded water structures in an aqueous solution [30]. At ranges of less than ~ 2–3 nm, to ignore this aspect of an aqueous solution can yield incorrect results. Finally, we must establish which PE headgroup conformational states permit the formation of interlipid and intralipid hydrogen bonds within the bilayer which is

in either a fluid or a gel phase. Our intention is to address the following questions: How many lipid–lipid hydrogen bonds per molecule are formed in the gel and fluid phases? What is the distribution of hydrogen bonds between the various moieties? How important is intralipid hydrogen bonding? Are hydrogen bond ''strings'' formed and, if so, how long are they and what is their structure? What effect does interlipid and intralipid hydrogen bonds have upon PE headgroup conformations and which are the most probable conformations to form hydrogen bonds? The intent of our calculation is to provide numbers for these quantities so that measurements can make comparisons with them.

Experimental work has shown that although there are many interlipid hydrogen bonds formed in the ''dehydrated crystalline'' (AS, anhydrous solid) phase, these are likely to be disrupted when water is added to create gel and fluid phases [3]. Hence, an expectation is that, while there are about four hydrogen bonds per dilauroylphosphatidylethanolamine (DLPE) molecule in the AS phase, this number is very much smaller in the other two phases. No direct measurements have yet been reported. Recently, a sequence of papers appeared which provide a review of most of the important recent work done on modelling PE-bilayer membranes [28,29]. These papers concerned themselves with ''minimal'' models on lattices, and introduced a new model to describe hydrogen bonding and hydration in lipid bilayers, with an emphasis on bilayers composed of PE molecules. They were concerned with the effects of hydrogen bonding in the headgroup region upon the ''main'' hydrocarbon chain melting phase transition which is driven by the competition between the energy gained in a low-temperature hydrocarbon chain-ordered gel phase and the entropy gained in the high-temperature chain-disordered fluid phase [1].

In the most recent work, in common with earlier models, the model states accessible to the headgroup of a single PE molecule, located at a lattice site, comprised a number of vectors which could point from the site towards any nearest-neighbour site, and which represented orientational ''bonding'' states that could take part in the formation of a hydrogen bond. There was also an ''unbonding'' state which was not represented by a vector and which did not form a hydrogen bond [29]. Each of these states was characterised by an internal energy and a degeneracy. The ends of the vectors were labelled ''donor'' (representing the proton ''donating'' NH_3^+ group) and ''acceptor'' (representing the proton ''accepting'' PO_2^- group). Only a donor–acceptor pair which were attached to collinear vectors located on nearest-neighbour lattice sites could form a hydrogen bond. This model was used to study the thermodynamics of hydrogen bond formation and its effect upon the ''main'' lipid-bilayer phase transition of phospholipids with PE headgroups, obtain a phase diagram, and to study under which conditions a percolating cluster of interlipid hydrogen bonds would be formed.

In order to answer the questions raised above, we must develop a different model. If one wants to predict the details of headgroup behaviour such as the average orientation of the P–N electric dipole or the average thickness of the headgroup region, then a model of the conformational states available to the headgroups in a lipid-bilayer membrane must be considered. We have developed a simplified model for the headgroup conformations of PE and phosphatidylcholine (PC) lipids and used it to predict the average values of variables associated with headgroups, as well as the effects of electrostatic interactions between lipid bilayers and model ''polypeptide'' chains tethered to the lipid bilayer [31]. We shall use that model here. In the case of a PE headgroup, we identified 17 states which appeared to be the most important. Each headgroup conformational state possesses an NH_3^+ ''donor'' and a PO_2^- ''acceptor''. A hydrogen bond can be formed if the ''donor'' associated with one lipid molecule is orientated suitably with the ''acceptor'' on another site (or even its ''own'' acceptor, though this possibility never occurs). However, there is also the possibility that an NH_3^+ donor can form either an interlipid or an intralipid hydrogen bond with the *sn2* C=O group, which protrudes into the aqueous region.

We shall not be concerned with lipid hydrocarbon chain states and shall assume that the system is in the form of a bilayer either in the gel or the fluid phase. We shall ignore fluctuations in the effective cross-sectional areas of the lipid molecules. Our intent is to carry out Monte-Carlo simulations of this headgroup model, with the plane of the bilayer represented by a triangular lattice, in order to study the interplay between headgroup conformational states, electrostatic

interactions and the formation of hydrogen bonds.

Because of their directionality and short range, hydrogen bonds can form only when the donors and acceptors are sufficiently aligned and are sufficiently close together. In this context, ''sufficiently'' means that the N–H $\cdots$ O sequence must be nearly linear and that the distance between the PO_2 or the C=O moieties and the NH_3 moiety must be a few Angstroms [32]. In a previous work, this restriction was correlated with the hydrocarbon chain state of the lipid molecules by assuming that, in the simplified model, a hydrogen bond could form only if the two nearest-neighbour molecules were in their all-trans (ground) states and if the two headgroup vectors were collinear. In the model presented here, however, headgroup conformational states can bring the NH_3 moiety sufficiently close to either the PO_2 or the C=O moiety, whether the system is in a gel or a fluid phase. Here we shall explore the implications of this new model for hydrogen bond formation.

2. Theory and computer simulation

We represented the interface between the hydrocarbon chain region of a planar lipid bilayer and the aqueous solution by a (plane) triangular lattice. The *z*-axis is perpendicular to this plane which is located at $z = 0$. The space $z > 0$ is the region of the aqueous solution. Each site of the lattice is occupied by a lipid molecule, or by part of a lipid molecule, the hydrocarbon chain region of which extends into the space $z < 0$, and the polar group of which extends into the space $z > 0$. The area of the unit cell of the lattice was taken to be the cross section of a phospholipid molecule, possessing saturated hydrocarbon chains, in a gel phase, $\sim 41\,\text{Å}^2$.

2.1. Model of the PE headgroup

The model that we shall use has been discussed elsewhere [31] and we shall reiterate only those aspects essential for this paper. Fig. 1(A) shows a schematic drawing of part of a lipid molecule possessing an extended PE headgroup. The plane at $z = 0$ indicates the local boundary between the (upper) aqueous solution and the (lower) oily, hydrocarbon chain region. We chose the position of this interface to be approximately intermediate between the two C=O groups. The P–N dipole, of magnitude $\sim 20\,\text{D}$ [33], was approximated by a point dipole located at the midpoint, z_0, of the finite-size dipole (Fig. 1(B)). The instantaneous orientation and magnitude, as well as the value of z_0, depends upon the conformational state of the headgroup. A positive angle corresponds to a dipole pointing away from the bilayer. The lattice site with which this lipid is associated is indicated by ''+'' and is located at the CH group in the glyceride backbone, to which the headgroup is attached. The distance, *h*, measured from this CH group, represents the ''height'' of the headgroup. The value of z_0 is measured from $z = 0$. Conformational states of the polar group involved only the headgroup segment between the NH_3^+ group and the CH group in the glyceride backbone. These conformational states, to be listed below, define the location and orientation of a dipole vector with respect to the *z*-axis, but not in the *xy*-plane. In order to sufficiently account for the latter we defined 12 such directions, $\{(n-1)\pi/6,\ n = 1,\ldots,12\}$, shown in Fig. 1(C). A headgroup conformational state was then defined as one of the conformational states, below, together with one of the 12 orientations in the *xy*-plane. We chose 12 as the smallest number which allowed relaxation so that the system of dipoles did not get locked into domains unrepresentative of thermal equilibrium.

In the model of headgroup conformational states used here we represented all such states as two-dimensional representations and shown in Fig. 1(D) for a PE headgroup. There we see the NH_3^+ moiety (filled circle) at one end of the chain with the CH group at the other end, and the position of the PO_2^- in the middle (open circle) with the orientation of the two oxygens indicated. We took the angle between successive bonds to be $2\pi/3$ for simplicity. For some states, we also show a portion of the glyceride backbone with the C=O group. The conformational states shown here and labelled s_1 to s_{17} are all those not forbidden by steric hindrances within that headgroup. Such intralipid steric hindrances were identified by considering the true conformations of such a headgroup, and not simply the two-dimensional representations shown in Fig. 1. We did not concern ourselves with steric hindrances between headgroups located on different lattice sites. The bond around

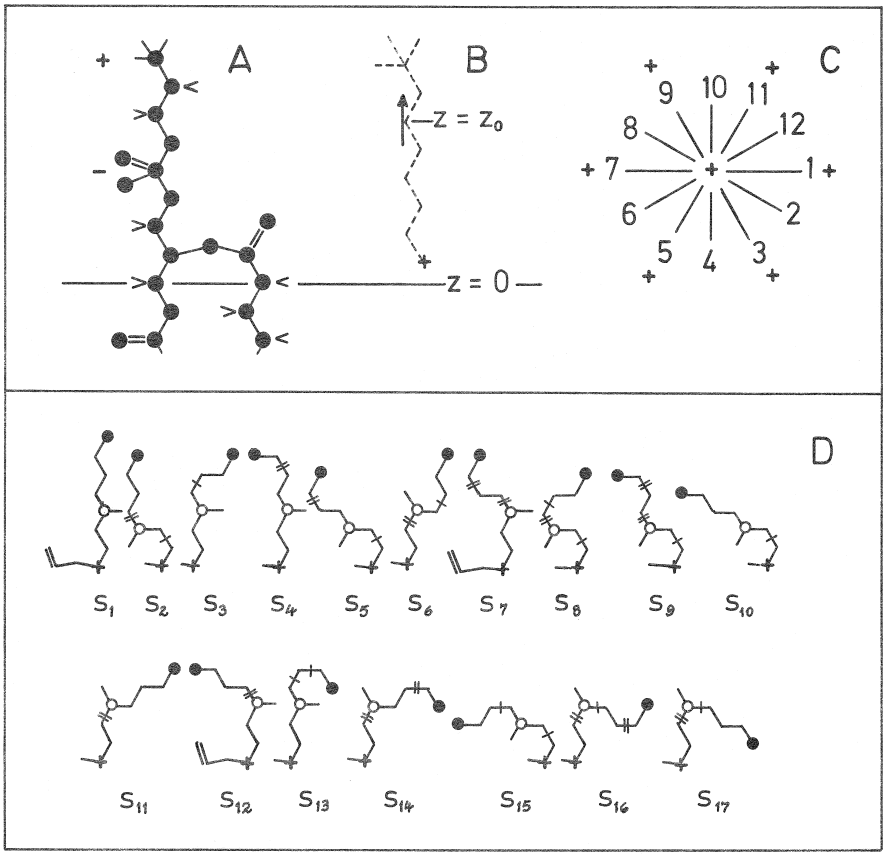

Fig. 1. (A) Schematic representation of a PE polar group in an extended conformation. The locations of the (+) and (−) charges are indicated. The horizontal line indicates the plane $z = 0$, the surface separating the hydrocarbon chain region ($z < 0$) and the aqueous region ($z > 0$). (B) Replacement of the finite dipole by a point dipole at $z_0 = (z_0(+) + z_0(-))/2$. The ''+'' indicates the CH group. (C) The 12 orientation states, in the plane of the bilayer, accessible to a headgroup. (D) Conformational states accessible by a PE headgroup. Solid circles indicate NH_3^+, open circles with a bar indicate PO_2^-, ''+'' indicates the CH group and ‖ indicates the C=O group in the glyceride backbone. Lines across bonds indicate that rotations around them have taken place. Double lines indicate a degeneracy twice that of rotations labelled by single lines. The values of $z(n)$ and the heights, $h(n)$, along the z-axis, are in units of bonds, each taken as 1.5 Å, which make an angle of $\pi/6$ with the z-axis. The length of each such unit is 1.299 Å. The value of $z(n)$ is the z-coordinate, measured from $z = 0$, of the centre of the P–N dipole. The height, $h(n)$, is measured from the CH moiety represented by a ''+'', and is the z-component of the distance along the z-axis, to the furthest extent of the headgroup. These distances are listed in columns two and five of Table 1.

which a rotation has taken place is indicated by a single or double line across it. The single line indicates that, because of steric hindrance, a rotation of $\sim \pm\pi/2$ is permitted, while the double line indicates a complete rotation of $\sim \pm\pi$ is possible. This enabled us to assign a relative degeneracy to these rotations, and we chose degeneracies to be: 1 for state s_1, 2 for bonds with single lines across them and 4 for those with a double line. These numbers are the correct orders of magnitude. Multiplicative factors of order unity are not going to change the general results obtained here because of the dominance of the electrostatic interactions. We stress that we are concerned only with a planar lipid bilayer.

Elsewhere [31], we were concerned with identifying headgroup conformational states which were too large to be accommodated within the plane of a lipid bilayer in its gel or fluid phases. To do so we defined an effective cross-sectional area of a headgroup, when it was in state s_n, to be $a_n = a_1 h(1)/h(n)$ where a_1 and $h(1)$ are the cross-sectional areas ($a_1 \approx 20.5$ Å^2) and heights of the headgroup in state s_1, and $h(n)$ is

the height of the headgroup when it is in state s_n. We chose $a_1 = 20.5\,\text{Å}^2$, because it is a single chain that, when extended, is approximately similar in cross section to a hydrocarbon chain. In our previous work [31], we allowed those states in Table 1 in gel phase calculations the cross-sectional areas of which were less than or equal to $41\,\text{Å}^2$, while all states with areas less than or equal to $62\,\text{Å}^2$ were admitted in calculations for a fluid phase. However, the average cross-sectional area of a saturated phospholipid in a region about 10° below the main phase-transition temperature is not the cross-sectional area of a pair of all-trans saturated hydrocarbon chains ($\sim 41\,\text{Å}^2$). Kink states with a cross-sectional area of $\sim 44\,\text{Å}^2$, for example, become probable in this temperature range and states with larger areas also cannot be ignored [23]. Accordingly, we estimated that a realistic average molecular cross-sectional area in this temperature region, in a gel phase, is $\sim 44\,\text{Å}^2$. We found, however, that PE headgroup states s_{15}, s_{16} and s_{17} possess values of a_n less than $\sim 48\,\text{Å}^2$. The radii associated with these two areas are $\sim 3.7\,\text{Å}$ and $\sim 3.9\,\text{Å}$, respectively. The difference in these two numbers is about 5%. The corresponding cross-sectional area of states s_9 and s_{10} of a PC polar group is $\sim 55\,\text{Å}^2$, giving a radius of $\sim 4.2\,\text{Å}$, a difference of $\sim 14\%$ when compared to the average radius of the gel state. Because the radius associated with the three PE states identified here is only 5% larger than the average radius in a gel phase, compared to those PC states for which the radius is 14% larger, we have admitted, in this paper, all PE headgroup states shown in Fig. 1(D) to both gel and fluid phases. We shall return to this point in the discussion.

Table 1 lists the values of the variables associated with the states, s_1 to s_{17}, each one identified by its values of $z_0(n)$, degeneracy, $D(n)$, electric dipole moment components, height, $h(n)$, and cross-sectional area (columns 2–6). Note that all degeneracies in column 3 are relative to the state s_1, with $D(1)$ defined to be unity. The units of distance used here are ''bond lengths'', while that of dipole moment

Table 1
States available to a PE polar group in the minimal model

State	$z_0(n)$ [a]	$D(n)$	Dipole moment components (bond length units)		$h(n)$ [a]	Cross-sectional area (Å^2)
			xy	*z*		
s_1	6	1	0	3.464	7	20.5
s_2	5	8			6	23.9
s_3	5.5	2			6	23.9
s_4	5.5	4			6	23.9
s_5	4.5	8			5	28.7
s_6	5.5	8	1.5	2.598	6	23.9
s_7	5.5	16			6	23.9
s_8	4.5	16			5	28.7
s_9	4.5	32			5	28.7
s_{10}	4	2			4	35.9
s_{11}	5	4	3.0	1.732	5	28.7
s_{12}	5	4			5	28.7
s_{13}	4.5	4	1.5	0.866	5	28.7
s_{14}	4	16	3.0	0	4	35.9
s_{15}	3	4	3.0	0	3	47.8
s_{16}	4	32	3.0	0	3	47.8
s_{17}	3	8	3.0	−1.732	3	47.8

[a] These are in units of ''bonds'', but not projected onto the *z*-axis via multiplication by $\cos(\pi/6)$ as in the case of the dipole moment *z*-component.

components is ''unit of electronic charge × bond length''. All bonds shown in Fig. 1 are taken to be of equal length, and chosen to be 1.5 Å.

Intralipid steric interactions have been taken into account explicitly by restrictions imposed on which headgroup conformational states which are accessible. Interlipid steric interactions have been taken into account, in an average way, by restricting which of those headgroup conformational states can be accessed in gel or fluid phases. Here, and previously [31], we either admitted or excluded states entirely. In early models of hydrocarbon chain packing in bilayers; however, a lateral pressure was used to represent such steric interactions. This approach gave results, e.g. Raman intensities in a gel phase, which were used to correctly predict subsequent measurements [23]. In Section 3, we shall consider an effective lateral pressure which can affect the probability of a state being occupied, and thus obtain results for thermal averages similar to those obtained by admitting or excluding states.

It should be noted that we have not assigned any internal energies, analogous to trans-gauche rotation energies of hydrocarbon chains. In carrying out the simulations, it became clear that the dominant considerations were the dipole–dipole interaction energies (below) and the restrictions as to which conformational states were accessible. In addition, we were not able to identify, with sufficient confidence, the energies associated with rotations about the bonds. Accordingly, we took them all to be equal.

We have represented the headgroup dipoles by point dipoles and can ask, how good is this approximation? To estimate this, we considered two cases:

(i) when a headgroup is in state s_1, we calculated the electric field strength at a neighbouring site, at a position away from the $z = 0$ plane corresponding to $z_0(1)$; and

(ii) the interaction energy between two parallel neighbouring dipoles, both in state s_{16} which is the most probably state found in both, the gel and fluid phases.

In case (i) we found that the electric field set up by the point dipole, pointing along **z** was ∼6% smaller than that set up by the two point charges at either end of the polar group dipole. In case (ii) we found that the energy of two parallel dipoles, arising from a pair of polar groups each in state s_{16}, aligned along the vector joining their sites, was about 19% weaker than the energy of the four charges associated with those two polar groups. Only in the gel phase did polar groups exhibit any short-range order in lining up parallel to each other, though, even in that case, the width of the distribution is ∼30°. It is likely that the error brought about by approximating the finite dipoles by point dipoles is, for most cases, ∼10% or less. In using point dipoles, then, it seems unlikely that our conclusions will be significantly modified by making use of the longer calculations involving point charges.

2.2. Dipole–dipole interactions and headgroup hydrogen bonding conformations and energies

In order to take into account the effect of dynamical hydrogen bonded clusters in the aqueous solution in calculating electrostatic energies, we made use of a non-local theory [30,34–39]. Such a mean-field theory represents instantaneous water structures by a time-averaged dielectric function. This approximation is justified since we are interested only in lipid conformational states which undergo small changes on time-scales slower than about 10^{-9} s and not in water structures which possess characteristic lifetimes in the 10^{-10}–10^{-11} s range. The physics of such a non-local theory depends upon the existence of dynamical hydrogen-bonded water structures: clusters of water molecules which form and disperse with a lifetime shorter than the characteristic time of molecular motion in a phospholipid membrane, viz. $\leq 10^{-9}$ s. We assume that, for short times, such clusters act like coherent structures: a force applied at one portion is transmitted with little damping across the structure. A consequence of this is that electric field effects at some point in an aqueous solution are due, not only to the electric field at that point, but also to electric fields in some neighbourhood (of a size characteristic of hydrogen-bonded water clusters) of that point. Mathematically, the difference between ''classical'' local and the ''non-local'' approach described here is the relationship between the polarization induced by a field at the site or by the fields at, and in the neighbourhood of, a site. Thus, the induced polarization vector, $\mathbf{P}(\mathbf{r})$, at point **r** is

$$\mathbf{P}(\mathbf{r}) = \epsilon(\mathbf{r})\mathbf{E}(\mathbf{r}) \quad \text{(local)} \tag{1a}$$

$$\mathbf{P}(\mathbf{r}) = \int \mathbf{d}^3\mathbf{r}'\epsilon(\mathbf{r},\mathbf{r}')\mathbf{E}(\mathbf{r}') \quad \text{(non-local)} \tag{1b}$$

where $\mathbf{E}(\mathbf{r})$ is the electric field at $\mathbf{r}$, $\mathbf{d}^3\mathbf{r}'$ is the infinitesimal volume in three-dimensions, $\epsilon(\mathbf{r})$ is the familiar ''classical'' permittivity (a local ''response function'') and $\epsilon(\mathbf{r},\mathbf{r}')$ can be referred to as the ''non-local'' permittivity (or response) function. In what follows, we make use of expressions for $\epsilon(\mathbf{r},\mathbf{r}')$ obtained elsewhere by using various approximations.

Elsewhere [30], it was shown that the electric field at position $\mathbf{R}$ in the aqueous solution, due to a point dipole, $\mathbf{P}_1$ located at $\mathbf{R}_0$ is

$$\mathbf{E}(\mathbf{P}_1,\mathbf{R}_0,\mathbf{R}) = \frac{1}{\epsilon_s}\sum_{j=1}^{2}\left\{3\frac{\mathbf{R}_j\cdot\mathbf{P}_1}{|\mathbf{R}_j|^5}\mathbf{R}_j g(|\mathbf{R}_j|) - \frac{\mathbf{P}_1 f(|\mathbf{R}_j|)}{|\mathbf{R}_j|^3}\right\},$$

$$g(|\mathbf{R}_j|) = \left(1 + k|\mathbf{R}_j| + \frac{1}{3}k^2|\mathbf{R}_j|^2\right)e^{-k|\mathbf{R}_j|} + \beta_j\left(1 + n|\mathbf{R}_j| + \frac{1}{3}n^2|\mathbf{R}_j|^2\right)e^{-n|\mathbf{R}_j|},$$

$$f(|\mathbf{R}_j|) = (1 + k|\mathbf{R}_j|)e^{-k|\mathbf{R}_j|} + \beta_j(1 + n|\mathbf{R}_j|)e^{-n|\mathbf{R}_j|}, \quad (2)$$

where

$$\mathbf{R}_1 = \mathbf{R} - \mathbf{R}_0, \qquad \mathbf{R}_2 = \mathbf{R} + \mathbf{R}_0, \qquad \mathbf{R}_0 = z_0\mathbf{z}, \quad (3)$$

$$\beta_1 = c_1, \quad \beta_2 = -c_1c_2, \quad c_1 = \frac{\epsilon_s}{\epsilon_\infty} - 1,$$

$$c_2 = \frac{\sqrt{\epsilon_s} - \sqrt{\epsilon_\infty}}{\sqrt{\epsilon_s} + \sqrt{\epsilon_\infty}}.$$

Here, k^{-1} and n^{-1} are the Debye shielding length, and a length characterizing water–water hydrogen-bond correlations, respectively. As before, we chose $k^{-1} = 1\,\text{nm}$ and $n^{-1} = 0.33\,\text{nm}$. The free energy of this system which accounts for the entropy of the electrolyte in a mean field way [40] is

$$F = -\frac{1}{2}\sum_{\mathbf{R}}\sum_{\mathbf{R}'}\mathbf{P}_{\mathbf{R}}\cdot\mathbf{E}(\mathbf{P}_{\mathbf{R}'},\mathbf{R}',\mathbf{R}), \quad (4)$$

where $\mathbf{P}_{\mathbf{R}}$ is the electric dipole at $\mathbf{R}$ and $\mathbf{E}(\mathbf{P}_{\mathbf{R}'},\mathbf{R}',\mathbf{R})$ is given in Eq. (2). Although Eq. (4) is a ''free energy'' in the sense that it includes the entropy of the electrolyte, it includes only the energetic terms of the dipole–dipole interactions between headgroups. It does not include the degeneracies of the various states of Table 1, nor does it include configurational entropy. We shall refer to this function as an ''energy'' while retaining the notation of F. The configurational entropy will be taken into account by the Monte Carlo procedure, while the degeneracies of the headgroup conformational states will be taken into account by adding to F (Eq. (5) below) a term of the form $-k_BT\ln(D(n))$, for a given headgroup in its conformational state s_n.

It should be noted that the effect of the non-local interaction is to extend the range of the electrostatic interactions which have been reduced by the Debye shielding [31]. This becomes more important as the value of z_0 increases. The result of ignoring the non-local interaction and consequent weakening of the electrostatic interactions is that the entropic terms in the free energy become more important, and conformational states which are oriented away from the bilayer plane increase their probability of occupancy. This means that $\langle\theta\rangle$ will increase as will the average distances, away from the bilayer plane, of some of the headgroup moieties. This was simulated and confirmed elsewhere [31].

When a phospholipid bilayer is in a gel phase, the lipid molecules occupy, approximately, the sites of a triangular lattice. Accordingly, we represented the plane of the hydrocarbon-chain–aqueous-solution interface as a triangular lattice [31]. Each site represents a lipid molecule and, thus, each site is occupied by one headgroup. Such a packing is approximately what occurs at temperatures $\sim 10^\circ$C below T_m. In a fluid phase, the area per lipid is ~ 62–$65\,\text{Å}^2$ compared to ~ 41–$45\,\text{Å}^2$ when the system is in a gel phase – a difference of $\sim 50\%$ [1]. In a fluid phase then, instead of one site per lipid, we should permit each lipid to occupy ~ 1.5 sites, so that each headgroup is associated with ~ 1.5 sites. Previously, we chose to implement this by requiring that two nearest-neighbour lipids, the headgroups of which occupy single sites, share a third site, which is not occupied by a headgroup and which is adjacent to the two headgroup-occupied sites [31]. We referred to this set of three sites occupied by two headgroups as a ''triad''. There are three configurations for a triad: two equilateral triangles and a straight line, and we distributed the headgroups randomly in this way. In practice, we were not able to cover the entire lattice

in this way, and the last ~5% of the headgroups were distributed randomly, but not strictly, in accord with the constraint imposed above. Since we represented the plane of the bilayer by a lattice, we did not consider making the distribution of headgroups on the lattice more, or less, sparse than what we used because then the headgroup density would be incorrect. We assumed that we were in a region sufficiently far from the main transition so that fluctuations in cross-sectional area were small. The lattice constant is, thus, always the diameter of a lipid molecule in a gel phase, ~0.72 nm.

A recent work by Zhang et al. [28] discussed various values for the energy of a hydrogen bond, E_h, formed between an NH_3 proton donor and oxygen proton acceptors on nearest-neighbour PE headgroups, compared to the energy of forming hydrogen bonds with water molecules. They arrived at a value of $\sim -2.2\times10^{-13}$ erg. A value of -3.9 kcal/mol ($\sim -2.7\times10^{-13}$ erg), a number somewhat higher than that chosen by Zhang et al., is quoted for an N–H $\cdots$ O hydrogen bond [33]. The latter energy, however, is not the value compared to the energy gained by forming hydrogen bonds with water and so should be higher than that found by Zhang et al. [28]. A value as low as $\sim -0.2\times10^{-13}$ erg, however, were deduced from experimental results [41]. This last figure is the average hydrogen bond energy per PE headgroup, and not necessarily the energy of a single PE–PE hydrogen bond. The wide divergence in the values can be reconciled, for example, if only 10% of the PE molecules form hydrogen bonds on the average, each of energy $\sim -2.1\times10^{-13}$ erg compared to the energy of forming hydrogen bonds with water. One of our intentions is to establish the value of E_h for PE polar groups. To do so, we studied values of E_h, ranging from -2.8×10^{-13} erg to -0.21×10^{-13} erg, and we shall report on four of them, namely -2.8, -2.1, -1.4 and -0.9×10^{-13} erg.

The total energy of the system, including the entropies of the electrolyte and the conformational states of the headgroups will then be given by the energy function,

$$E(F,\{s_n\},N_h) = F - k_B T \sum_i \sum_n \ln\big(D(n)\big) L_{in} - E_h N_h, \qquad (5)$$

where F is given in Eq. (4), L_{in} is a projection operator for the lipid headgroup at site i and is unity if the lipid is in state s_n and zero otherwise, and N_h is the total number of hydrogen bonds formed each of energy E_h. The hydrogen bond energies are assumed to be additive. The set $\{s_n\}$ represents the set of headgroup conformational states occupied. There are relatively few conformational states in which headgroups can form hydrogen bonds. In this model, for example, intralipid hydrogen bonds cannot be formed since the headgroup cannot access a conformation whereby its NH_3 group can form a hydrogen bond with either of the phosphate or carbonyl groups on the same molecule. The interlipid hydrogen bonds can be deduced by considering the conformations shown in Fig. 2. Table 2 lists all the pairs and it can be seen that a PO_2 acceptor attached to a headgroup in any conformational state can bond to a nearest-neighbour NH_3 donor only in states s_{10}, s_{14}, s_{15}, s_{16} and s_{17}. Thus, for example, an acceptor in state s_{14} can bond only to a donor in state s_{10}, while an acceptor in s_1 can bond to a donor in any one of states s_{10}, s_{14}, s_{15}, s_{16}. The only exception is s_{15} with which no acceptor can form a hydrogen bond. In the case of bonding to the C=O group, the donor states are even more restricted as shown in Table 2.

It is useful to compare the electrostatic energies with those of hydrogen bonds. The electrostatic interactions of each molecular dipole with its 90 nearest

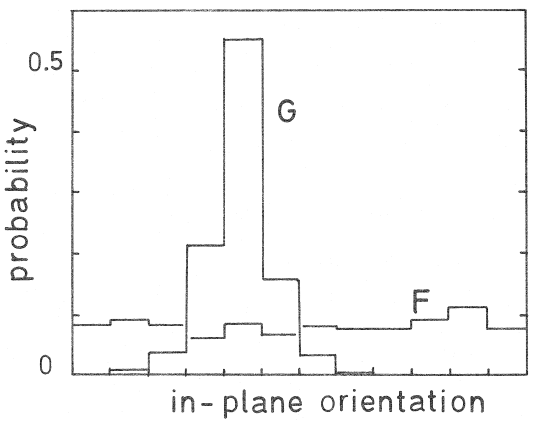

Fig. 2. Probabilities of finding the P–N dipole moment component in the plane of the bilayer, for the 12 directions considered, in the gel (G) and fluid (F) phases. $E_h = -0.9\times10^{-13}$ erg, $k = 0.1$ Å^{-1} and $n = 0.3$ Å^{-1}. The direction of the maximum of the gel phase distribution is not unique.

Table 2
States which may form interlipid hydrogen bonds pairwise as indicated

Acceptor state	Donor state
Bonding to PO_2^-	
1, 3, 4, 7, 12, 13	10, 14, 15, 16
2, 5, 8, 9, 10	15, 17
6, 11, 14, 16, 17	10
15	–
Bonding to C=O	
(a) All except 15	17
(b) All	15, 17

The states, s_n, are indicated only by their subscript n. In the cases of bonding to PO_2^- and C=O (case (a)) groups, the headgroups must be nearest neighbours and must be oriented so that the angle between them, projected onto the local bilayer plane, must not be more than $\pi/3$. In case (b) of bonding to a C=O group, the long axes of nearest-neighbour lipid molecules must be at right angles.

neighbours was computed and used in the simulation and the resulting number was, as expected, of order unity. The inclusion of further dipoles gave corrections of order 10^{-6}. The average electrostatic energy per lipid dipole, when the system was in equilibrium, was $\sim -4.1\times10^{-13}$ ergs (gel phase) and $\sim -2.9\times10^{-13}$ ergs (fluid phase). The negative sign shows that it is attractive. This should be compared to the average hydrogen bond energy per lipid dipole of $\sim -0.2\times10^{-13}$ ergs which arises from the energy of -0.9×10^{-13} ergs of an individual hydrogen bond. It should be recalled that the ''hydrogen bond energy'' is actually the difference between the free energies of forming hydrogen bonds between a pair of nearest-neighbour headgroups and two headgroups forming hydrogen bonds with water in the aqueous solution.

2.3. Monte-Carlo simulation

We made use of the Metropolis algorithm [42]. Eq. (5) includes the dipole–dipole electrostatic energies, the hydrogen bond energies, the degeneracies (entropies) of single-headgroup states and the entropy of the electrolyte. The simulation procedure itself accounts for the configurational entropy of the system.

One ''Monte-Carlo (MC) step'' involved the following: Each lipid headgroup was visited in a random sequence. The energy of the system (5), $E(F,\{s_n\},N_h)=E$, was calculated and a site, i, was randomly selected. A new conformational state was selected for the headgroup and a check was made as to whether existing hydrogen bonds must be broken, or whether new hydrogen bonds could be formed. When we simulated fluid phases, we also attempted to exchange randomly selected pairs of ''triads'' (above). The new energy, $E(F',\{s'_n\},N'_h)=E'$, was calculated. It was assumed that if a new hydrogen bond could be formed, then it would be formed. In cases in which the donor could form a bond with either of two acceptors (PO_2^- or C=O), one of them was chosen randomly. This choice is of significance for the calculation of the relative intensities of spectral bands. The energy difference, $\Delta E = E' - E$, was used in the Metropolis algorithm to decide whether the new state was accepted. Implementation of the Monte-Carlo method involved initializing the system, using an arbitrary initial state, for a sufficiently large number of MC steps (see below) in order to obtain a state characteristic of thermal equilibrium. After this, averages of quantities of interest were calculated by carrying out a sufficiently large number of MC steps (see below) and computing the average from the sequence of instantaneous values obtained. We used triangular lattices of size $(30)^2$ and $(72)^2$ with periodic boundary conditions, and we initialized the states of the lipid dipoles for 10 000 steps and then computed averages for 20 000 to 40 000 steps. We found no significant difference between the results for the two lattices and all the results presented here are for $(30)^2$ lattices. We calculated the probabilities for lipids with PE headgroups to lie in the various states in gel and fluid phases. From these, thermodynamic averages, such as the average heights and xy- and z-components of the headgroup dipole moments, were calculated. We found later that initialization and average-computing for 5000 MC steps each, yielded results in agreement with the much longer runs.

3. Results and comparison with experiment and discussion

The simulations were carried out at temperatures, T, of 300 K (gel phase) or 340 K (fluid phase). We

Table 3
Probabilities and thermodynamic averages for a PE polar group in gel and fluid phases with $k = 0.1\,\text{Å}^{-1}$, $n = 0.3\,\text{Å}^{-1}$ and $E_h = -0.9\times10^{-13}$ erg

Quantity	Gel	Fluid
$p(10)$	0.062	0.042
$p(14)$	0.215	0.195
$p(15)$	0.065	0.069
$p(16)$	0.428	0.387
$p(17)$	0.150	0.170
$\langle P_z \rangle$ (D)	0.1	1.0
$\langle \theta \rangle$ (deg)	0.4	2.8
N (Å)	5.0	5.1
$CH_2(\beta)$ (Å)	4.9	5.0
$CH_2(\alpha)$ (Å)	4.8	4.9
O (Å)	5.3	5.3
P (Å)	5.0	5.0
$\Delta\nu_Q(\beta)$ (kHz)	7.3	5.7
$\Delta\nu_Q(\alpha)$ (kHz)	7.1	4.9
p_h (PO_2^-)	0.073	0.046
p_h(C=O)	0.160	0.170
f_{h-}	0.071	0.087
f_{h+}	0.072	0.088
τ_h (MC steps)	14.1	11.5
$\langle E_h \rangle$ (10^{-13} erg)	−0.21	−0.19

The states s_n are indicated only by their subscripts n. Shown here are the probabilites for the dominant conformational states, 10, 14, 15, 16, 17; the average z-component of dipole moment; the average angle of the dipole moment away from the bilayer plane; the average positions of the P, O, CH_2 α and β, and N with respect to the hydrocarbon-chain–aqueous-solution interface at $z = 0$; ^{2}H NMR quadrupole spittings for the α and β CH_2 groups assuming sufficiently rapid averaging around the axis perpendicular to the local bilayer plane; the probabilites for hydrogen bond formation (p_h) with the phosphate or carbonyl groups; the fraction of hydrogen bonds broken (f_{h-}) or formed (f_{h+}) per MC step and the average lifetime per hydrogen bond; the average hydrogen bonding energy (relative to that with water).

searched for the value of E_h which yielded an average value, $\langle E_h \rangle$, close to that of ~ -0.3 kcal/mol ($\sim -0.2\times10^{-13}$ erg) obtained by Shin et al. [41]. We found that $E_h = -0.9\times10^{-13}$ erg gave $\langle E_h \rangle = -0.21\times10^{-13}$ erg from results obtained for the gel phase and $\langle E_h \rangle = -0.19\times10^{-13}$ erg from results for the fluid phase. Table 3 shows the results for the headgroup and hydrogen bond statistics in the fluid and gel phases. Rather than list all the states, for some of which the probabilities are irrelevantly small, we have listed probabilities for only the most populated states. In both phases there are five dominant states: s_{10}, s_{14}, s_{15}, s_{16} and s_{17}, the probabilities of which sum to at least 0.86. There are, however, two dominant states, s_{14} and s_{17}, for which the P–N dipole is either parallel to the bilayer plane (s_{14}) or points towards the hydrocarbon chain region making an angle of 30° with the bilayer plane (s_{17}). These distributions give the average value of the angle θ, $\langle \theta \rangle$, that the P–N dipole makes with the local plane of the lipid bilayer to be $\sim 0°$ in the gel phase and $\sim 3°$ in the fluid phase. This leads to a z-component of dipole moment of ~ 1 D (fluid phase) which decreases to ~ 0.1 D in the gel phase. The average distances of the five groups near the end of the headgroup, P, O, $CH_2(\alpha)$, $CH_2(\beta)$ and N, from the $z = 0$ plane lie between 4.8 Å and 5.3 Å with the result that the P–N dipole is nearly parallel to the bilayer plane in both phases. This results in calculated ^{2}H NMR quadrupole splittings for the α and β CH_2 groups of 4.9 and 5.7 kHz (fluid phase) and 7.1 and 7.3 kHz (gel phase). respectively These results were calculated on the assumption of sufficiently rapid rotation around the z-axis. We have been unable to find experimental results for these quantities in pure PE bilayers. However, they are similar to fluid phase results of 5.8 and 5.9 kHz (C_α in DMPC and POPC) and 5.0 kHz (C_β in DMPC) [43,44].

Fig. 2 shows averages of the instantaneous distribution of the dipole components parallel to the plane of the bilayer (in-plane) for both the gel (G) and fluid (F) phases. It is clear that while the bilayer exhibits no long-range order in the fluid phase, all directions being equally probable, the gel phase does possess a net dipole moment. It is seen that the gel phase in-plane distribution exhibits a full-width-at-half-height of ~ 40–$50°$.

The probabilities for finding an $NH_3\cdots PO_2$ or an $NH_3\cdots C{=}O$ hydrogen bond, $p_h(PO_2^-)$ and p_h(C=O), were calculated to be 0.073 and 0.160 (gel phase) and 0.046 and 0.170 (fluid phase), respectively. We also calculated the fraction of hydrogen bonds at each MC step that were broken, f_{h-}, and formed, f_{h+}, in the fluid and gel phases and found them to be 0.071 and 0.072 (gel phase), and 0.087 and 0.088 (fluid phase), respectively. The lifetime of a hydrogen bond, τ_h, was defined to be the average number of successive MC steps for which the bond

remained unbroken, and we found τ_h to have values of 14.1 MC steps (gel) and 11.5 MC steps (fluid). These numbers can be converted to seconds if one can identify the ''time elapsed per MC step''. It should not be assumed that this elapsed time is the same in both the gel and fluid phases.

We are able to compare our results for p_h(C=O) with experiments carried out by Lewis and McElhaney [13]. They measured the C=O infrared stretching band intensities in the 1650–1800 cm^{-1} region, comparing results for DMPE with DMPC in both the fluid and gel phases (Fig. 6 of [13]). They found that, while one could account for the DMPC spectrum with two overlapping bands, an understanding of the DMPE band required an additional, third, band centred at $\sim$1705–1710 cm^{-1}. Since the C=O groups of both the PC and the PE can take part in hydrogen bonding with water, but only the PE can form interlipid hydrogen bonds involving the C=O groups, the third band can be interpreted as a C=O stretch when the carbonyl is involved in hydrogen bonding with a PE moiety. If this interpretation is correct, then the relative intensities of the third band in the fluid and gel phases should be given by the ratio of the two calculated values of p_h(C=O) for the fluid and gel phases. From Table 3 we see that this ratio is 1.06. The ratio calculated from Fig. 6 of [13] is $\sim$1.25. We feel that the agreement is satisfactory.

We have calculated the fraction of C=O groups taking part in interlipid hydrogen bonding: Table 3 shows that this lies between 0.16 (gel) and 0.17 (fluid) of the C=O groups on the *sn2* chain. It is not easy to identify the appropriate band in the data of Fig. 6 of [13], but, if it is assumed that the area under the curves is proportional to the number of groups taking part in the different kinds of hydrogen bonding, then we find that the fraction is $\sim$0.8 (fluid) and $\sim$0.6 (gel). These numbers are substantially larger than our calculations and it is possible that either our ''minimal'' model is insufficiently accurate or that we have over interpreted the data of [13].

Table 4 shows the dominant headgroup conformational states together with the 2-state probabilities for hydrogen bond formation between one headgroup donating a proton (columns) and another molecule accepting it at either the PO_2 or the C=O groups (rows), in both the gel (G) and fluid (F) phases. It can be seen that state s_{17} is by far the dominant proton-donor conformation, with the dominant proton acceptor states being s_{14}, s_{16} and s_{17}. That states s_{10} and s_{15} are donors but not acceptors can be seen from Fig. 1(D): the PO_2 acceptor is not easily accessible and even the C=O group is ''covered'' by the headgroup.

Fig. 3 shows an instantaneous configuration, at MC step 20 000, of the $(30)^2$ lattice in the gel (A) and fluid (B) phases. The double-dots indicate headgroups which do not possess PE–PE hydrogen bonds, the axis of the two dots indicating the headgroup orientation projected onto the plane of the bilayer. Integers indicate headgroups which possess such hydrogen bonds, the integer indicating the conformational state (0 represents state s_{10}, 2 – state s_{12},..., 7 – state s_{17}) and its orientation indicating the in-plane orientation of the headgroup. Solid lines joining integers indicate the hydrogen bond locations. Two things are clear: (i) the hydrogen bond ''strings'' are short (1–4 in the gel phase and 1–3 in the fluid phase); and (ii) the hydrogen bond orientation exhibits long-range order in the gel phase, mimicking the order of the in-plane dipole moment orientation, while the hydrogen bonds exhibit no such order in the fluid phase. It must be remembered that, while there are 900 headgroups shown in the gel phase, there are 600 in the fluid phase because not all sites are occupied by headgroups (see above for the model of the fluid phase). Accordingly, the fraction of headgroups taking part in hydrogen bonding is nearly equal in both phases. We have not distinguished between PO_2 and C=O acceptors.

Table 5 shows the probabilities of finding the five headgroup moieties, P, O, $CH_2(\alpha)$, $CH_2(\beta)$ and N at various distances above the plane $z = 0$ (see Fig. 1). These distances are ''quantized'', since the conformations shown in Fig. 1(D) have access to only certain positions (in units of ''bond lengths'' of 1.5 Å projected onto the z-axis, yielding distances in units of 1.3 Å) away from the plane $z = 0$. One could superimpose Gaussians on each discrete value with the area under the Gaussian associated with a given position equal to the probability value associated with that position. These distributions can be used to analyze neutron scattering from a lipid bilayer to establish whether the calculations are consistent with measurements. It can be seen that while the P and O groups exhibit small fluctuations, the two CH_2 groups

Table 4
Probabilities for a hydrogen bond to be formed when a PE headgroup is in the states indicated

Acceptor molecule	Donor molecule									
	10		14		15		16		17	
	G	F	G	F	G	F	G	F	G	F
12	–	–	0.04	–	–	–	0.07	0.05	–	–
14	0.05	–	–	–	0.04	–	–	–	0.12	0.14
16	0.09	0.05	–	–	0.09	0.09	–	–	0.25	0.28
17	0.05	–	–	–	0.07	0.07	–	–	0.10	0.11

The states s_n are indicated only by their subscripts n. Note that this includes bonds formed with a carbonyl group which is attached to the glyceride backbone. For gel (G) and fluid (F) phases with $k = 0.1\,\text{Å}^{-1}$, $n = 0.3\,\text{Å}^{-1}$ and $E_h = -0.9 \times 10^{-13}$ erg.

appear to exhibit a broader double-peaked distribution. In the fluid phase, the distribution of the positions of the nitrogen ranges from 2.6 to 10 Å with a maximum at 5.2 Å and two local maxima at 2.6 and 7.8 Å. In the gel phase, the nitrogen exhibits almost as large position fluctuations as it does in the fluid phase.

In order to estimate the validity of admitting all PE headgroup states to calculations in both the fluid and gel phases, we considered the effect of including an additional term in the energy function Eq. (5). If the cross-sectional area of a state, a_n, was more than some area, A_{gel}, representing the cross-sectional area of the hydrocarbon chain region of a single lipid

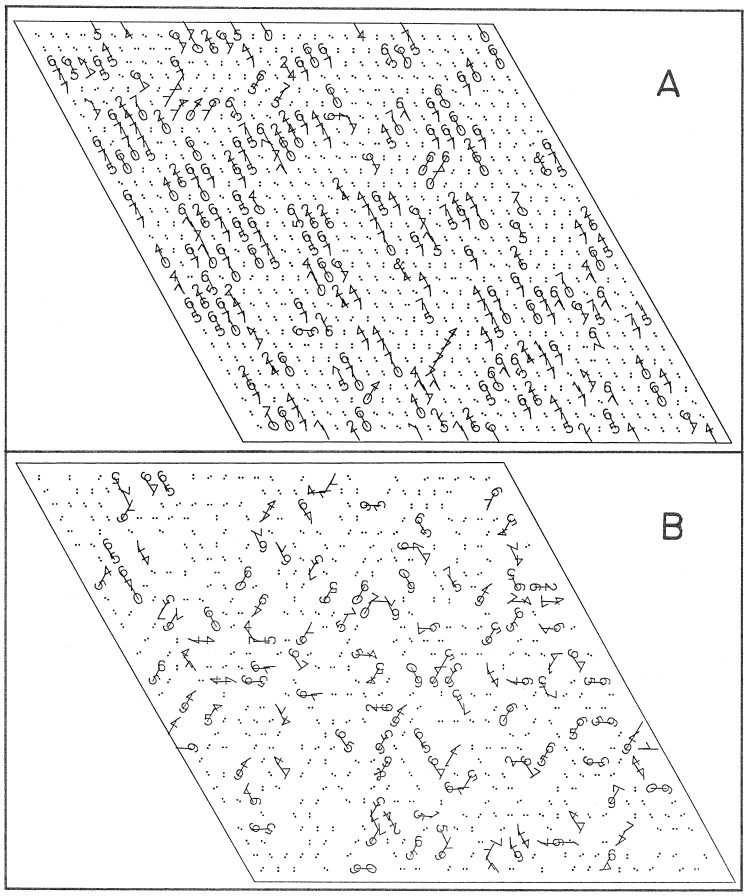

Fig. 3. Instantaneous distributions of those headgroup conformational states involved in hydrogen bond formation, P–N in-plane (i.e. in the plane of the bilayer) orientations and hydrogen bonds in the gel (A) and fluid (B) phases. $E_h = -0.9 \times 10^{-13}$ erg, $k = 0.1\,\text{Å}^{-1}$ and $n = 0.3\,\text{Å}^{-1}$. Conformational states s_{10}, s_{12}, s_{14}, s_{15}, s_{16} and s_{17} are indicated by integers 0, 2, 4, 5, 6 and 7 and the orientation of the integer shows the in-plane P–N orientation. Headgroups not forming hydrogen bonds are indicated by · · with the orientation indicating the in-plane direction of the headgroup. Hydrogen bonds formed are indicated by solid lines connecting the integers.

Table 5
Spatial distribution of the five headgroup moieties

Phase	Distance from $z = 0$ (Å)	Probabilities for finding moiety at distance				
		P	O	$CH_2(\alpha)$	$CH_2(\beta)$	N
	10.4	–	–	–	–	0.00
	9.1	–	–	–	0.00	0.02
	7.8	–	–	0.01	0.09	0.11
Fluid	6.5	–	0.06	0.31	0.28	0.05
	5.2	0.83	0.94	0.21	–	0.58
	3.9	0.17	–	0.56	0.63	0.07
	2.6	–	–	–	–	0.17
	9.1	–	–	–	0.00	0.01
	7.8	–	–	0.00	0.05	0.07
Gel	6.5	–	0.05	0.29	0.30	0.06
	5.2	0.86	0.95	0.13	–	0.64
	3.9	0.14	–	0.58	0.65	0.07
	2.6	–	–	–	–	0.15

Probabilities for finding P, O, $CH_2(\alpha)$, $CH_2(\beta)$ and N at various distances from $z = 0$ (Fig. 1(A)) for $E_h = -0.9\times10^{-13}$ erg, $k = 0.1\,\text{Å}^{-1}$ and $n = 0.3\,\text{Å}^{-1}$, in fluid and gel phases. A value of 0.00 indicates a probability less than 0.01 but not identically 0.

molecule in the gel phase, then a term was added to the energy function Eq. (5),

$$\Pi(a_n - A_{\text{gel}}), \tag{6}$$

where Π is an effective lateral pressure acting in the headgroup region. If a_n is less then A_{gel} then no such term was added. We chose $\Pi = 30$ dyne/cm, since this is approximately the effective lateral pressure acting on hydrocarbon chains, and $A_{\text{gel}} = 44\,\text{Å}^2$ (see above). This term adds a small, but non-trivial, energy to states s_{15}, s_{16} and s_{17}. The results of further simulations showed that all probabilities for finding states, n, to be occupied, $p(n)$, changed by ≤ 0.001 except for $p(14)$ and $p(16)$. In a gel phase these changed to 0.246 and 0.387 from 0.215 and 0.428, respectively, while in a fluid phase they changed to 0.223 and 0.350 from 0.195 and 0.387, respectively (see Table 3). These changes, however, affected thermodynamic quantities slightly. The angle that the P–N group makes with the bilayer plane, $\langle\theta\rangle$, changed to 0.7° from 0.5° (gel) and to 3.5° from 2.7° (fluid). The positions, along the z-axis, of the two CH_2 groups in the headgroup changed by ~ 0.1 Å to lie further from the hydrocarbon layer region. The probabilities, $p_h(PO_2^-)$ and $p_h(C{=}O)$ changed from those given in Table 3 to 0.074 and 0.159 (gel phase), and to 0.046 and 0.170 (both unchanged) (fluid phase), respectively. These results show that we may include the states s_{15}, s_{16} and s_{17} in calculations for both the gel and fluid phases.

Finally, we can remark on the results obtained if we make the hydrogen bond energy, E_h, stronger. If we choose $E_h = -1.4\times10^{-13}$ erg (~ -2 kcal/mol), then the most probable state is still s_{16} with $p(16) = 0.32$ (gel) and 0.31 (fluid) resulting in $\langle\theta\rangle = -1.8°$ (gel) and 0° (fluid). The probabilities of forming hydrogen bonds become 0.43 (gel) and 0.38 (fluid) and the average hydrogen bond energy becomes $\langle E_h\rangle \approx -0.5\times10^{-13}$ erg (~ -0.7 kcal/mol). If we set $E_h = -2.1\times10^{-13}$ erg, however, then the most probable state becomes s_{17} with $p(17) = 0.38$ (gel) and 0.40 (fluid) resulting in $\langle\theta\rangle = -4.8°$ in both phases. The probabilities of forming hydrogen bonds become 0.62 (gel) and 0.59 (fluid) and the average hydrogen bond energy becomes $\langle E_h\rangle \approx -1.2\times10^{-13}$ erg. With a stronger hydrogen bond, $E_h = -2.8\times10^{-13}$ erg (~ -4 kcal/mol), then we find that s_{17} remains the most probable state with $p(17)$ increasing to 0.47 (gel) and 0.53 (fluid) resulting in $\langle\theta\rangle = -7.2°$ (gel) and $-9.5°$ (fluid). The probabilities of forming hydrogen bonds increases to 0.74 in both gel and fluid phases and the average hydrogen bond energy becomes $\langle E_h\rangle \approx -2.1\times10^{-13}$ erg (~ -3 kcal/mol).

4. Conclusions

We have used a model of lipid headgroup conformational states [31] in order to study hydrogen bond statics in phospholipid bilayers with PE headgroups. All 17 states described elsewhere [31] were used and, because of the similarity of their cross-sectional areas compared to that of the hydrocarbon chain segment, no restrictions, which depended upon the effective cross-sectional area of the hydrophobic region of the lipids, projected onto the plane of the bilayer, were imposed. Steric hindrances were accounted for by hard-core repulsions within a headgroup as it changed its conformational state. We represented the dipoles of the headgroups as point dipoles in order to simplify the calculation of electrostatic interactions be-

tween them. We used a non-local theory of electrostatic interactions, which includes Gouy–Chapman theory as one limiting case, and takes into account, in a mean-field way, the effects of hydrogen bonding in the aqueous medium.

We represented the plane of the bilayer by a triangular lattice, each site of which corresponded to an area of $\sim 41\,\text{Å}^2$, characteristic of the projection onto the plane of the bilayer, of a lipid in a gel phase with the hydrocarbon chains oriented perpendicular to the bilayer plane. We did not consider ripple or tilted phases. In a gel phase, therefore, one lipid headgroup was associated with each lattice site. In a fluid phase, where the average cross-sectional area of a lipid molecule is $\sim 62\,\text{Å}^2$, each molecule would occupy, on average, ~ 1.5 lattice sites. We ignored fluctuations by imposing the condition that each headgroup is always associated with ~ 1.5 sites with the site unoccupied by a headgroup being a nearest neighbour of two headgroup-occupied sites, between which it is shared. The validity of this model has been discussed in detail elsewhere [31].

We assumed that all hydrogen bonds formed between any NH_3^+ group and any PO_2^- or C=O group possessed the same energy. This energy, E_h, is relative to the energy of forming hydrogen bonds between water and the pair of groups which are involved in lipid–lipid hydrogen bonding. Since we were unable to assign, a priori, the strength of the attractive hydrogen bond energy, we considered six cases: $E_h = -0.5,\ -0.7,\ -0.9,\ -1.4,\ -2.1$ and -2.8 in units of 10^{-13} ergs. The largest energy is approximately that quoted for an N–H $\cdots$ O bond [32]. We identified the value of E_h relevant to this system by requiring that its average value, $\langle E_h \rangle = E_h \langle N_h \rangle / N_L$, where $\langle N_h \rangle$ is the average number of hydrogen bonds formed and N_L is the number of lipid molecules, be equal to the value measured by Shin et al. [41]. We modelled infinitely-large homogeneous domains of gel- and fluid-phase lipids and represented them by $(30)^2$ lattices with periodic boundary conditions. Our results are as follows:

1. We found that a value of $E_h = -0.9 \times 10^{-13}$ erg gave $\langle E_h \rangle = -0.21 \times 10^{-13}$ erg from results obtained for the gel phase and $\langle E_h \rangle = -0.19 \times 10^{-13}$ erg from results for the fluid phase, in agreement with the measurements of Shin et al. [41].
2. Five states in the both, the gel and the fluid phases account for $\geq 86\%$ of the probability of occupying any of the 17 headgroup conformational states. These are states s_{10}, s_{14}, s_{15}, s_{16} and s_{17}.
3. We calculated the probabilities for finding the headgroup moieties, P, O, $CH_2(\alpha)$, $CH_2(\beta)$ and N, to lie a given distance from the plane $z = 0$ (Fig. 1(D) and Table 5). In both phases, the O lies furthest from the hydrocarbon chain layer (average distance $\sim 5.3\,\text{Å}$) with the PO_2 and NH_3 groups lying next at $\sim 5\,\text{Å}$. This results in the P–N dipole lying nearly parallel to the bilayer plane in both phases. This result should be observable via neutron scattering. The thickness of the headgroup layer undergoes essentially no change on going from the gel to the fluid phase.
4. We found that the distributions of nitrogen positions, in both the gel and fluid phases, exhibited strong peaks around 5.2 Å, with much smaller peaks around 2.6 and 7.8 Å. Also in both phases, the two CH_2 groups exhibited narrower, double-peaked distributions. Only the O and the PO_2 exhibit a narrow single peak.
5. Our results for the relative number of C=O groups on the *sn2* chain taking part in interlipid hydrogen bonding in the fluid phase compared to the gel phase is 1.06 which compares well with the ratio of ~ 1.25 deduced from the data of [13]. The ratio of such groups taking part in interlipid hydrogen bonding compared to water hydrogen bonding in each phase was calculated to lie between 0.16 and 0.17. With some assumptions, the results of [13] might suggest that this number is ~ 0.6–0.8.
6. The most likely combinations of nearest-neighbor headgroup conformational states forming hydrogen bonds are: 17 $\rightarrow$ 14 and 17 $\rightarrow$ 16 in both phases. Significant contributions also come from 17 $\rightarrow$ 17 and 15 $\rightarrow$ 16, with weaker contributions coming from 16 $\rightarrow$ 12, 15 $\rightarrow$ 17, 15 $\rightarrow$ 14 (gel), 14 $\rightarrow$ 12 (gel), 10 $\rightarrow$ 14 (gel), 10 $\rightarrow$ 16 and 10 $\rightarrow$ 17 (gel). Here $X \rightarrow Y$ means that a headgroup in state s_X donates a proton from its NH_3 group to form a hydrogen bond with either a PO_2^- or a C=O of a nearest-neighbour headgroup in state s_Y.
7. PE headgroups, in a homogeneous gel phase, exhibit dipolar orientational long-range order in the plane of the bilayer. The distribution of orientation

angles exhibited a full width at half height of between $\sim 40°$ and $\sim 50°$. A fluid phase exhibits no such order.

8. The formation of interlipid hydrogen bonds has been invoked as a reason for the higher value of the ''main'' transition temperature of PE bilayers compared to PC bilayers possessing the same hydrocarbon chains. We have found, however, that the number of hydrogen bonds do not differ substantially between the fluid and gel phases. Our conclusion, therefore, is that this model is unlikely to display any significant effect of hydrogen bonding upon the ''main'' hydrocarbon chain melting phase transition at T_m, except, possibly, a broadening of any hysteresis, compared to the case of PC bilayers where interlipid hydrogen bonding is absent. If this is correct then, the cause of the higher main transition temperature of PE bilayers compared to PC bilayers, with the same hydrocarbon chains, must be sought elsewhere. It should be borne in mind, that the headgroup conformational states accessible by a PE headgroup differ from those accessible by a PC headgroup [31].

Many of the numerical values of the quantities reported here might be measured using neutron or infrared techniques. We are in the process of modelling lipid bilayers composed of a mixture of lipids with PE and phosphatidylcholine (PC) headgroups. Our intention is to predict the changes in the average number of hydrogen bonds as a function of PC concentration. Should this model prove to be adequate to predict quantities, then we shall use it to model hydrogen bonds formed between macromolecules, at the interface of a lipid bilayer and an aqueous solution, and lipid headgroups.

Acknowledgements

This work was supported by NSERC of Canada (DAP, MJZ) and FCAR (MJZ). We would like to thank two reviewers who raised some important points.

References

[1] G. Cevc, D. Marsh, Phospholipid Bilayers. Physical Principles and Models, Wiley, New York, 1987.
[2] J.R. Silvius, P.M. Brown, T.J. O'Leary, Biochemistry 25 (1986) 4249.
[3] J.N. Israelachvili, Intermolecular and Surface Forces, Academic Press, London, 1985.
[4] J. Boggs, Can. J. Biochem. 52 (1980) 3425.
[5] H. Hauser, I. Pascher, R.H. Pearson, S. Sundell, Biochim. Biophys. Acta 650 (1981) 21.
[6] P.B. Hitchcock, R. Mason, K.M. Thomas, G. Shipley, Proc. Natl. Acad. Sci. U.S.A. 938 (1974) 3036.
[7] J.M. Seddon, K. Harlos, D. Marsh, J. Membr. Biol. 258 (1983) 3850.
[8] H. Chang, R.M. Epand, Biochim. Biophys. Acta 728 (1983) 319.
[9] J.R. Silvius, Chem. Phys. Lipids 57 (1991) 241.
[10] J.M. Seddon, G. Cevc, D. Marsh, Biochemistry 22 (1983) 1280.
[11] D.A. Wilkinson, J.F. Nagle, Biochemistry 23 (1984) 1538.
[12] H.H. Mantsch, S.C. Hsi, K.W. Butler, D. Cameron, Biochim. Biophys. Acta 728 (1983) 325.
[13] R.N.A.H. Lewis, R.N. McElhaney, Biophys. J. 64 (1993) 1081.
[14] H.E. Alper, D. Bassolino-Klimas, T.R. Stouch, J. Chem. Phys. 99 (1993) 5547.
[15] H. Heller, M. Schaefer, K. Schulten, J. Phys. Chem. 97 (1993) 8343.
[16] S.-J. Marrink, M. Berkowitz, H.J.C. Berendsen, Langmuir 9 (1993) 3122.
[17] K.V. Damodaran, K.M. Merz, Biophys. J. 66 (1994) 1076.
[18] A.J. Robinson, W.G. Richards, P.J. Thomas, M.M. Hann, Biophys. J. 67 (1994) 2345.
[19] K. Tu, D.J. Tobias, M.L. Klein, Biophys. J. 69 (1995) 2558.
[20] U. Essmann, L. Perera, M.L. Berkowitz, Langmuir 11 (1995) 4519.
[21] K. Tu, D.J. Tobias, M.L. Klein, J. Phys. Chem. 99 (1995) 10035.
[22] K. Tu, D.J. Tobias, J.K. Blaisie, M.L. Klein, Biophys. J. 70 (1996) 595.
[23] D.A. Pink, T.J. Green, D. Chapman, Biochemistry 19 (1980) 349; R.G. Snyder, D.G. Cameron, H.L. Casal, D.A.C. Compton, H.H. Mantsch, Biochim. Biophys. Acta 684 (1982) 111.
[24] A. Hussin, H.L. Scott, Biochim. Biophys. Acta 897 (1987) 423.
[25] K.A. Dill, D. Stigter, Biochemistry 27 (1988) 3446.
[26] A.L. MacDonald, D.A. Pink, Phys. Rev. B 37 (1988) 3552.
[27] M.K. Granfeldt, S.J. Miklavic, J. Phys. Chem. 95 (1991) 6351.
[28] Z. Zhang, J. Tobochnik, M.J. Zuckermann, J. Silvius, Phys. Rev. E 47 (1993) 3721.
[29] J. Tobochnik, M.J. Zuckermann, Z. Zhang, Phys. Rev. E 51 (1995) 6204.
[30] M. Belaya, V. Levadny, D.A. Pink, Langmuir 10 (1994) 2015.
[31] D.A. Pink, M. Belaya, V. Levadny, B. Quinn, Langmuir 13 (1997) 1701.
[32] See, e.g., T. Moeller, Inorganic Chemistry, A Modern Introduction, Wiley, New York, 1982, p. 251 et seq.

[33] M. Thompson, W.H. Dorn, in: T.E. Edmonds (Ed.), Chemical Sensors, Blackie, Glasgow and London, 1988.
[34] A.A. Kornyshev, in: R.R. Dogonadze, E. Kalman, A.A. Kornyshev, J. Ulstrup (Eds.), The Chemical Physics of Solvation, Elsevier, Amsterdam, 1985.
[35] M.L. Belaya, V.G. Levadny, M.V. Feigelman, Sov. Phys. JETP 64 (1986) 787.
[36] G. Cevc, Chem. Scr. 25 (1986) 96.
[37] M.L. Belaya, M.V. Feigelman, V.G. Levadny, Chem. Phys. Lett. 126 (1986) 361.
[38] M.L. Belaya, M.V. Feigelman, V.G. Levadny, Langmuir 3 (1987) 648.
[39] A.A. Kornyshev, D.A. Kossakowski, M.A. Vorotyutsev, in: M.P. Tosi, A.A. Kornyshev (Eds.), Condensed Matter Physics. Aspects of Electrochemistry, World Scientific, Singapore, 1991.
[40] L.D. Landau, E.M. Lifshitz, Electrodynamics of Continuous Media, Pergamon Press, Oxford, 1960.
[41] T.-B Shin, R. Leventis, J.R. Silvius, Biochemistry 30 (1991) 7491.
[42] N. Metropolis, A.W. Rosenbluth, M.N. Rosenbluth, A.H. Teller, E. Teller, J. Chem. Phys. 21 (1953) 1087.
[43] J. Seelig, P.M. Macdonald, P.G. Scherer, Biochemistry 26 (1987) 7535.
[44] A. Watts, L.C.M. van Gorkom, in: P. Yeagle (Ed.), The Structure of Biological Membranes, CRC Press, Boca Raton, 1992.